

Andrzej Czarski*, Piotr Matusiewicz*

SOME ASPECTS OF ESTIMATION ACCURACY OF MEAN TRUE INTERLAMELLAR SPACING

1. INTRODUCTION

Pearlite is a product of eutectoid reaction in Fe-Fe₃C system. A lamellar morphology of parallel ferrite and cementite plates within colonies is dominating [1–3].

A lamellar microstructure is quantitatively characterized by interlamellar spacings. The following denotations are used: l_t – true interlamellar spacing, l_r – random interlamellar spacing and l_a – apparent interlamellar spacing.

The full stereological description of lamellar microstructure consists in estimating of distribution of the true interlamellar spacing on the ground of the apparent interlamellar spacing or the random interlamellar spacing [4–6].

In practice – for example during examinations of the relationships between microstructure and properties – considering a lamellar microstructure it is sufficient to determine a mean true interlamellar spacing \bar{l}_t [7–9]. The accuracy of \bar{l}_t determining is the subject of this work.

2. MEASUREMENT OF LAMELLAR MICROSTRUCTURE

Measureable parameters of the lamellar microstructure are the number of random spacings per length L of secant i.e. $N(L)$ as well as random interlamellar spacing l_r and apparent interlamellar spacing l_a . The measurement of the l_r spacing is made on a random secant (it is the \overline{ac} intercept length), the l_a spacing in the point corresponds to the \overline{ab} intercept length (Fig. 1). The methodology of measuring the l_r and l_a spacings is presented in the work [10].

* Ph.D.: AGH University of Science and Technology, Faculty of Metals Engineering and Industrial Computer Science, Krakow, Poland; e-mail: czarski@agh.edu.pl

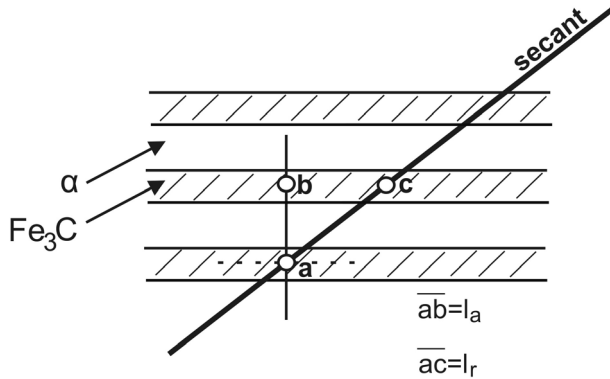


Fig. 1. Measureable parameters of the lamellar microstructure: random interlamellar spacings l_r and apparent interlamellar spacing l_a

To measure the parameters of lamellar microstructure we can use image analysis methods [9]. The principle of measuring the apparent interlamellar spacing l_a was presented by Lafond and others [11] as well as Camard and others [12] a long time ago. It consists in comparison of two identical images of the microstructure. Executing the successive translations of a one image into another the area of covering plate intersections of the specified phase is registered; l_a spacing corresponds to a translation vector length guaranteeing the maximum area of covering intersections.

The usability of SigmaScan Pro image analyzer in a semi-automatic measurement of lamellar microstructure was presented by Matusiewicz and others [9].

The interesting alternative for computer image analysis is measurement of l_a spacing using the coherent light effect technique. In 1982 Stiebler and others [13] as first demonstrated the method of a mean l_a spacing determination using a device working on the basis of a scheme of the Joung experiment in a laser version. A measurement using this method was carried out on lamellar Pb-Sn eutectic obtained as a result of directional crystallization. The described method was later developed and modified by among others Fitta [14].

3. SOME STEREOLOGICAL RELATIONSHIPS FOR LAMELLAR MICROSTRUCTURE

Gensamer [15] and next the others (DeHoff [4], Underwood [5], Saltykow [16]) determine the mean random spacing \bar{l}_r as follows:

$$\bar{l}_r = 1/\bar{N}_L \tag{1}$$

where \bar{N}_L – the mean density of intersections of secant with plates of specified phase (in case of pearlite – with cementite plates).

A full probabilistic interpretation of Eq. (1) was given by Czarski and Ryś [17, 18]:

$$\bar{l}_r = E^{-1}(l_r^{-1}) \quad (2)$$

where $E(\cdot)$ is expected value.

According to Eq. (1), the mean random interlamellar spacing \bar{l}_r is the estimator of the reciprocal of the expected value $E(l_r^{-1})$. By analogy we define [17, 18]:

- the mean apparent interlamellar spacing \bar{l}_a :

$$\bar{l}_a = E^{-1}(l_a^{-1}) \quad (3)$$

- the mean true interlamellar spacing \bar{l}_t :

$$\bar{l}_t = E^{-1}(l_t^{-1}) \quad (4)$$

Taking into account Eq. (1), Eq. (2) and Eq. (4) the relations between the mean interlamellar spacings $\bar{l}_t, \bar{l}_r, \bar{l}_a$ are as follows [4–6, 16–18]:

$$\bar{l}_r = 2\bar{l}_t \quad (5)$$

$$\bar{l}_a = \frac{4}{\pi}\bar{l}_t \quad (6)$$

After linearization of adequate functions of random variables we can determine standard deviations of mean interlamellar spacings \bar{l}_r, \bar{l}_a (and in consequence the estimation margin of error of \bar{l}_t):

- $N(L)$ – number of intersections of secant with cementite plates (number of random spacings l_r) per secant length L – is an elementary (single) measurement:

$$s_{\bar{l}_r} = \frac{L s_{N(L)}}{N(L)^2 \sqrt{k}} \quad (7)$$

where:

- $s_{N(L)}$ – standard deviation of number of intersections per secant length L ,
- L – secant length,
- $\overline{N(L)}$ – mean number of intersections per secant of length L ,
- k – number of secants of length L ,

- random interlamellar spacing l_r is an elementary (single) measurement:

$$s_{\bar{l}_r} = \frac{s_{l_r^{-1}}}{\bar{l}_r^{-1} \sqrt{k}} \quad (8)$$

where:

$s_{l_r^{-1}}$ – standard deviation of reciprocal of random interlamellar spacing,

\bar{l}_r^{-1} – mean of reciprocal of random interlamellar spacing,

k – number of interlamellar spacings l_r ,

- apparent interlamellar spacing l_a is an elementary (single) measurement:

$$s_{\bar{l}_a} = \frac{s_{l_a^{-1}}}{\bar{l}_a^{-1} \sqrt{k}} \quad (9)$$

where:

$s_{l_a^{-1}}$ – standard deviation of reciprocal of apparent interlamellar spacing,

\bar{l}_a^{-1} – mean of reciprocal of apparent interlamellar spacing,

k – number of interlamellar spacings l_a .

4. EXPERIMENTAL PROCEDURE

4.1. Subject of experimental investigations, material

The aim of the investigations is to show the methodology of accuracy of the mean true interlamellar spacing \bar{l}_l estimation.

A high-purity Fe-Fe₃C alloy has been used for experiment. The chemical composition of the alloy and heat treatment parameters carried out to produce a coarse lamellar pearlite microstructure were presented earlier [10]. Obtained lamellar microstructure is presented in Figure 2.

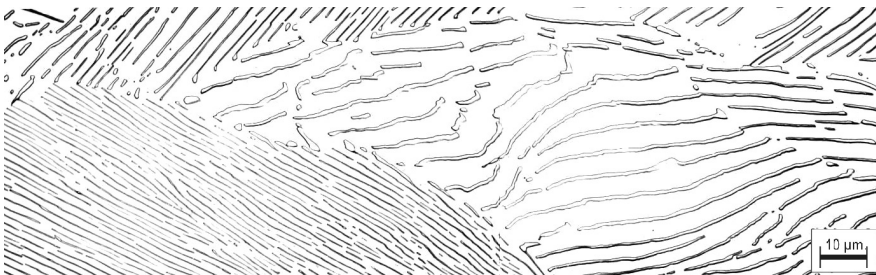


Fig. 2. Microstructure with coarse lamellar pearlite (etched in picral)

4.2. Preliminary quantitative description of microstructure

Within the framework of a preliminary quantitative estimation of the microstructure the relative volume of areas where cementite was non-lamellar was determined (there are usually clusters of cementite particles) i.e. $V_{v(np)}$. Regarding this estimation it was necessary to accept the criterion enabling to distinguish a shape “plate – not plate” (a particle) on the basis of a flat cut shape. It is impossible to formulate an objective criterion, but there are some arbitral criteria. Chattopadhyay and Sellars [19] assume that an object cut by a random plane is a plate if the ratio of its length to thickness exceeds 8:1. While according to Chojnowski and Tegart [20] this ratio should be more than 5:1 to admit that the object is a plate.

Estimation of volume fraction of area with non-plate cementite was carried out by means of lineal analysis [4, 5], the 8:1 criterion was accepted, the result: $V_{v(np)} = 0.029 \text{ mm}^3/\text{mm}^3$.

4.3. Accuracy of mean true interlamellar spacing \bar{l}_t estimation

The measurements of all parameters ($N(L)$, l_r , l_a) have been carried out at total magnification 2500 \times . The errors, (absolute $\delta_{\bar{l}_t}$ and relative $\gamma_{\bar{l}_t}$) were calculated with the 95% confidence level assumption.

Elementary measurement $N(L)$

Random secants of length $L = 200 \text{ mm}$ were projected over the lamellar microstructure ($k = 420$). On each secant the number of intersections with plates and cementite particles were counted. The results of measurements are presented in Figure 3 and in Table 1.

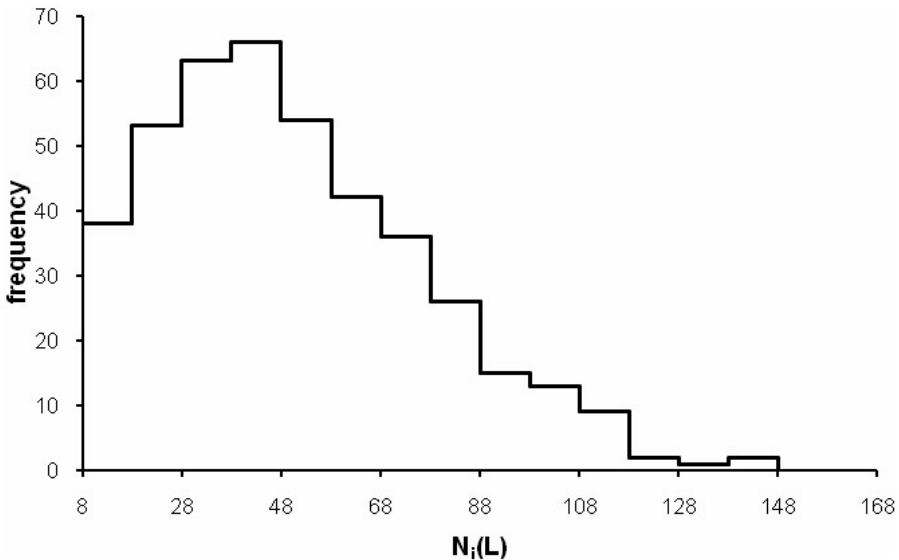


Fig. 3. Empirical distribution of number of intersections on the secant of length L , $N(L)$ ($L = 0,08 \text{ mm}$)

Table 1. Results of measurements; elementary measurement – $N(L)$

k	$\overline{N(L)}$	$s_{N(L)}$	$\overline{l}_r \cdot 10^3$	$s_{\overline{l}_r} \cdot 10^3$	$\overline{l}_t \cdot 10^3$	$\delta_{\overline{l}_t} \cdot 10^3$	$\gamma_{\overline{l}_t}$
			[mm]	[mm]	[mm]	[mm]	[%]
420	50.81	26.80	1.57	0.041	0.787	0.040	5.04

Elementary measurement – l_r

The measurement of random interlamellar spacing l_r has been performed on a random secants. Accuracy of a single measurement was $0.2 \cdot 10^{-3}$ mm, that corresponds to 0.5 mm at 2500× magnification. Detailed description of the measurement method has been presented earlier [10]. The results of measurements are presented in Figure 4 and in Table 2.

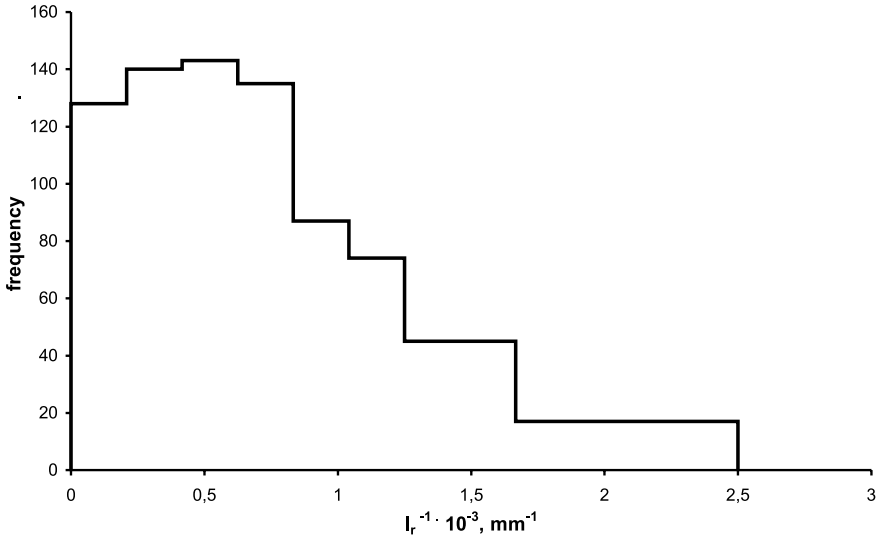


Fig. 4. Experimental distribution of random interlamellar spacing inverse, \overline{l}_r^{-1}

Table 2. Results of measurements; elementary measurement – l_r

k	$\overline{l}_r^{-1} \cdot 10^{-3}$	$s_{\overline{l}_r^{-1}} \cdot 10^{-3}$	$\overline{l}_r \cdot 10^3$	$s_{\overline{l}_r} \cdot 10^3$	$\overline{l}_t \cdot 10^3$	$\delta_{\overline{l}_t} \cdot 10^3$	$\gamma_{\overline{l}_t}$
	[mm ⁻¹]	[mm ⁻¹]	[mm]	[mm]	[mm]	[mm]	[%]
890	0.647	0.437	1.545	0.035	0.773	0.034	4.44

Elementary measurement – l_a

The measurement of an apparent interlamellar spacing l_a has been performed according to methodic presented earlier [10]. Accuracy of a single measurement was $0.2 \cdot 10^3$ mm,

that corresponds to 0.5 mm at 2500× magnification. The results of measurements are presented in Figure 5 and in Table 3.

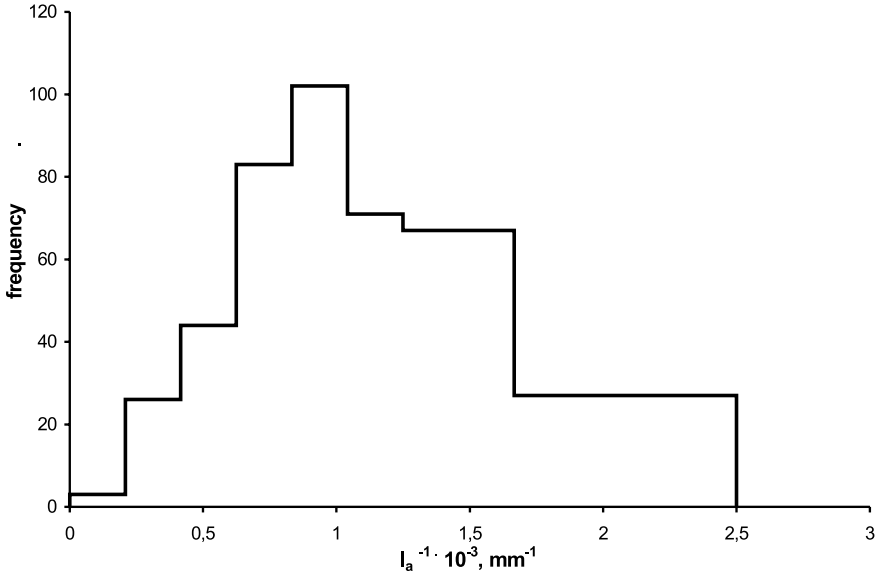


Fig. 5. Experimental distribution of apparent interlamellar spacing, $\overline{l_a^{-1}}$

Table 3. Results of measurements; elementary measurement – l_a

k	$\overline{l_r^{-1}} \cdot 10^{-3}$	$s_{l_r^{-1}} \cdot 10^{-3}$	$\overline{l_r} \cdot 10^3$	$s_{\overline{l_r}} \cdot 10^3$	$\overline{l_t} \cdot 10^3$	$\delta_{\overline{l_t}} \cdot 10^3$	$\gamma_{\overline{l_t}}$
	[mm^{-1}]	[mm^{-1}]	[mm]	[mm]	[mm]	[mm]	[%]
432	0.998	0.431	1.002	0.021	0.787	0.032	4.07

5. DISCUSSION

The mean values of random interlamellar spacing $\overline{l_r}$ obtained on the basis of $N(L)$ and l_r are very close (Tabs 1, 2). Insignificant higher value of $\overline{l_r}$ is observed in case of counting $N(L)$ (Tab. 1). This difference can be explained by the fact that the counting included also non-lamellar areas i.e. (according to the accepted criterion) cementite particles.

The accuracy of estimation of true interlamellar spacing using all the three methods is comparable and sufficient (in each case a relative estimation error was not more than 5%). To achieve such a result it was necessary to carry out a significant number of measurement (counts).

Acknowledgements

The financial support from the Polish Ministry of Science and Higher Education (MNiSW) contract No. 11.11.110.082 is gratefully acknowledged.

REFERENCES

- [1] *Hillert M.*: The formation of pearlite, in: Zakay V.F., Aaronson H.I. (Eds.), *Decomposition of austenite by diffusional processes*, NY Interscience, New York, 1962, 197–237
- [2] *Hackney S.A., Shiflet G.J.*: Pearlite growth mechanism, *Acta Metall.*, 35 (1987), 1019–1028
- [3] *Doi S.N., Kestenbach H-J.*: Determination of the pearlite nodule size in eutectoid steels, *Metallography*, 23 (1989), 135–146
- [4] *Underwood E.E.*: *Quantitative Stereology*, Addison-Wesley, 1970
- [5] *DeHoff R.T., Rhines F.N.*: *Quantitative Microscopy*, McGraw-Hill, New York, 1968
- [6] *Vander Voort G.F., Roos A.*: Measurement of the interlamellar spacing of pearlite, *Metallography*, 17 (1984), 1–17
- [7] *Ikeda T., Ravi V.A., Snyder G.J.*: Evaluation of true interlamellar spacing from microstructural observations, *Journal of Materials Research*, 23 (2008), 2538–2544
- [8] *Elwazri A.M., Wanjara P., Yue S.*: Measurement of pearlite interlamellar spacing in hypereutectoid steel, *Materials Characterization*, 54 (2005), 473–478
- [9] *Matusiewicz P., Czarski A., Adrian H.*: Quantitative Microstructure Analysis with SigmaScanPro, Proc. of 9th ECSIA & 7th Stermat, 2005, 131–138
- [10] *Czarski A., Glowacz E.*: Relationship between mean values of interlamellar spacings in Case of Lamellar Microstructure Like Pearlite, *Archives of Metallurgy and Materials*, 55 (2010), 101–105
- [11] *Lafond C., Moliexe F.*: Some metallurgical applications of stereometry, *Practical Metallography*, spec. iss., 5 (1975), 200–223
- [12] *Camard P., Chermant J.L., Coster M.*: Morphology of an imbricate structure, *Practical Metallography*, spec. iss. 8 (1978), 126–132
- [13] *Stiebler K., Otte B., Frebel M., Nembach E.*: Investigation of periodic lamellar substructures by laser beam diffraction., *Mat. Sc. and Eng.*, 56 (1982), 203–209
- [14] *Fitta G.*: Dyfrakcyjna metoda ilościowej analizy struktur typu płytkowego, AGH – Wyzd. Metalurgiczny, Kraków, 1985 (PhD thesis)
- [15] *Gensamer M., Pearsall E.B., Pellini W.S., Low J.R.*: Tensile properties of pearlite, bainite and spheroidite, *Trans. ASM*, 30 (1942), 983–1020
- [16] *Saltykov S.A.*: *Stereometric Metallography*, 3rd edition, Metallurgia, Moscow, 1970
- [17] *Ryś J., Czarski A.*: Quantitative analysis of lamellar structure, Proc. of IV Symposium on Metallography, Vysoke Tatry, Czechoslovakia, 1 (1986), 25–30
- [18] *Czarski A., Ryś J.*: Stereological relationships for lamellar structure, *Acta Stereologica*, 6 (1987), 567–572
- [19] *Chattopadhyay S., Sellars C.M.*: Quantitative measurements of pearlite spheroidization, *Metallography*, 10 (1977), 89–105
- [20] *Chojnowski E.A., Tegart W.J.*: Accelerated spheroidization of pearlite, *Metal Sc. J.*, 2 (1968), 14–18